Performance Analysis of Three-Phase Active Power Filter with Switched Mode Inverter

Dr. Mustafa M. Ibrahem
Associate Professor

Jabbar R. Rashed
M.Sc. Elec. Eng.

College of Engineering-Dept. of Electrical Engineering
University of Basrah

Abstract- This paper presents a simplified control method for three-phase active power filter by calculating the required reactive and harmonics current of the load. The active power filter needs this current to correct the power factor and eliminate the generated harmonics by nonlinear loads. This method has the advantages of using only one current sensor and effectiveness in achieving the required compensation characteristics. The proposed circuit may be operate at frequencies ranging from 40 to 60 Hz and it also responds very fast under sudden changes in the load conditions. The considered system is analyzed and a prototype is also developed and tested to demonstrate the performance of the implemented active power filter in the power factor improvement and harmonics elimination. Finally, predicted results are verified experimentally.

Index Terms: Reactive power, harmonics, active power filters, pulse-width modulation.

تحليل أداء مرشح القدرة الفعال ثلاثي الطور ذو النمط المفتاحي

الخلاصة:

هذا البحث يقدم طريقة سيطرة مبسطة لأحد مرشحات القدرة الفعال ثلاثي الطور عن طريق حساب التيار غير الفعال والتوافقيات الموجودة في تيار الحمل. هذا التيار يحتاجه المرشح لتصحيح معامل القدرة وإزالة التوافقيات التي تتولد نتيجة وجود الأحمال غير الخطية. تمتاز هذه التقنية بحاجتها إلى متحسس واحد لتيار الحمل وفعاليتها في إنجاز الوظائف المطلوبة. الدائرة المقترحة تستطيع العمل في مديات من التردد تمتد من (40 – 60) هيرتز كما إنها تستجيب بسرعة كبيرة لتغيرات الحمل المفاجئة. لقد تم تحليل النظام المقترح ، كما تم بناء نموذج عملي وفحصه لتوضيح أداء مرشح القدرة الفعال المنفذ في تحسين معامل القدرة وإزالة التوافقيات. وأخيراً تم تفحص النتائج المتوقعة عملياً.

List of symbols

APF	Active power filter
VSI	Voltage source inverter
CSI	Current source inverter
PLL	Phase locked loop
PWM	Pulse width modulation
$i_l(t)$	Load current
I_d	Dc component of the load current
I_a	Active current amplitude
I_r	Reactive current amplitude
I_{2n}	Even harmonics current amplitude
I_{2m+1}	Odd harmonics current amplitude
ϕ_{2n}	Phase angle of the even harmonics component
ϕ_{2m+1}	Phase angle of the odd harmonics component
$i_a(t)$	Active component of the load current
$i_{rh}(t)$	Reactive component of the load current
ω	Mains frequency
α	Scaling factor of the analogue multiplier
K_p	Proportional parameter of the P – I controller
K_i	Integral parameter of the P – I controller
T_0	Time constant of the low pass filter
τ	Width of the generated pulses
T_s	Time period of the carrier signal
A_c	Amplitude of the carrier signal
$V_{inv.}(t)$	Output of the power inverter
V_{dc}	dc value of the pulses in the output of the power inverter
M	Modulation index
$i_F(t)$	The injected compensating current to ac line
L_f	Output inductance of the power inverter
$V_s(t)$	Mains voltage

1. Introduction

Nonlinear power electronic devices are extensively used in recent years, these loads act as several problems source. One of these problems is the low power factor, and the another problem is caused by the harmonics in the load current, which pollute the mains supply [1-2].

A conventional solution to reactive power compensation and harmonic cancellation is the use of passive filter. However, this kind of filter is not adequate due to their inability to compensate random frequency variations in the current and also can produce series and parallel resonance with source impedance. Thereby, this problem is partially solved with help of LC passive filters [3-5].

This paper presents one of the major development recently applied, namely, the active power filter. This filter has been proposed and developed to overcome problems of traditional methods. Whereas the active power filter (APF) generates the required reactive and harmonic current, therefore, the mains only needs to supply the fundamental current. This filter is voltage source inverter controlled as a current source by means of a pulse-width modulation (PWM) signal [3], [6].

The APF uses an inverter and a dc source to generate the required voltage or current waveform. This APF can be operated with two general types of inverter; voltage source inverter (VSI) or current source inverter (CSI) as shown in Figs. 1 and 2 respectively. Generally, the voltage source inverter is preferred for the active power filter because of its lower losses [4], [7].

This filter can compensate for a leading or lagging power factor without sensing and computing the associated reactive power component. Also, it attenuates the amplitude

compensate all the reactive power. There are two types of dc side of the inverter; storage dc capacitor or an independently controlled dc supply. Also, to reduce the current ripple and to limit drawn current from the filter, inductors are connected in filter branch

The general block diagram of three-phase active power filters is shown in Fig. 3.

IV. *The Control Strategy*

(a) Basic principle:

The block diagram of the proposed control circuit for active power filter (one phase) is shown in Fig.4 .Multiplying the given load current in equation (1) by (cosωt) results in equation (3):

$$i_1(t)\cdot\cos(\omega t) = I_d\cos(\omega t)+\frac{I_a}{2}+\frac{I_a}{2}\cos(2\omega t)+\frac{I_r}{2}\sin(2\omega t)+\sum_{n=1}^{\infty}\frac{I_{2n}}{2}\left[\cos((2n+1)\omega t+\Phi_{2n})+\cos((2n-1)\omega t+\Phi_{2n})\right]+\sum_{m=1}^{\infty}\frac{I_{2m+1}}{2}\left[\cos((2m+2)\omega t+\Phi_{2m+1})+\cos((2m-2)\omega t+\Phi_{2m})\right] \quad \ldots(3)$$

In equation (3), the only $I_a/2$ term is proportional with the magnitude of the active component and it can be extracted by using the control circuit as shown in Fig. 4. In this circuit, the cut-off frequency of the low pass filter is chosen below the lowest frequency component of the line current. Therefore, the complete attenuation from (ω) to up gives a good estimation of the active current amplitude (I_a). Then, the estimated amplitude (I_a) is multiplied by a unity sinusoid in-phase with line voltage to obtain an excellent estimation of the active current i_a (t). Being estimated, it is fed with the measured load current to summing node to generate the required reactive and harmonic currents.

To analyze the circuit shown in Fig. 4, assume it has reached a steady state condition, i.e., the output of the summing node will be as stated in equation (2). Then, by definition and agreement $i_{rh}(t)$ should not have an active component because it is subtracted from the load current $i_l(t)$. After multiplication with (cosωt), no dc component will be present, as can be observed in equation (3) by letting I_a=0. This means that the ΔI_a (as shown in Fig. 4) will be zero, which will keep constant the output of the P-I controller, i.e, I_a. Finally, the out put of the P-I controller will exactly correspond to the magnitude of the active current $i_a(t)$ if the load current is not changed.

Also, a PLL circuit is used to implement the line voltage in-phase sinusoid generator block, (shown in Fig.4). The PLL technique has two features; on is the phase tracking of the line voltage over operating frequency range (40-60) Hz, and the another is that this circuit blocks efficiently the distortion in the line voltage to generate a clean sinusoid wave.

(b) System model:

The circuit in section(a) can be represented in s-domain as shown in Fig. 5. The open loop transfer gain of this circuit:

$$G(S)=\frac{\alpha^2(K_pS+K_I)}{S(T_oS+1)} \quad \ldots(4)$$

Also, the closed loop transfer function of the control circuit can be drive as follows:

$$I_{rh}(S) = I_l(S) - I_a(S) \quad \ldots(5)$$

and

$$I_a(S) = G(S)\,.\,I_{rh}(S) \quad \ldots(6)$$

of the current harmonic components generated by nonlinear loads.

This paper presents a new control technique of the APF, which has three unique features. One is using simple and accurate circuits such as only one load current sensor and PLL estimation circuit. The another advantage it is very fast under sudden change in load condition and the third feature, this method can operate successfully in wide range of frequencies. These advantages contribute to achieve the unity power factor and give a minimum acceptable level of the harmonic distortion.

In this work, theoretical analysis and experimental investigations of the characteristics of the system are presented and feasibility of the proposed technique is verified.

II. *General Description of the System*

The formed load current by the power factor and harmonics is made up of the following four terms:

$$i_l(t) = I_d + I_a\cos(\omega t) + I_r\sin(\omega t) + \sum_{n=1}^{\infty} I_{2n}\cos(2n\omega t + \phi_{2n}) + \sum_{m=1}^{\infty} I_{2m+1}\cos((2m+1)\omega t + \phi_{2m+1}) \quad \ldots(1)$$

The first term in equation (1), which represents the dc component, is usually small or it does not exist at all. The only component that the mains should supply is the active current ($I_a\cos\omega t$), which is really the second term whereas the third term ($I_r\sin\omega t$) stands for the reactive current. The other two final terms comprise the even and odd harmonic components in the load current respectively. If the active power filter supplies the dc, reactive and harmonic currents to the load, so the mains needs only to supply the active current. This can be easily accomplished by subtracting the active current $i_a(t)$ from the measured load current $i_L(t)$ as follows:

$$i_{th}(t) = i_l(t) - i_a(t) = i_l(t) - I_a\cos(\omega t) \quad \ldots(2)$$

Where $i_{th}(t)$ clearly enough represents all the components in the load current except the active component. From equation (2), it can be noticed that I_a is the magnitude of in-phase current (which needs to be estimated) and ($\cos\omega t$) is the sinusoid in-phase with respect to line voltage. To achieve the experimental realization of equation (2), two sensors are needed, the first one is to detect the load current and the other to sense the mains voltage.

III. *The proposed three-phase APF*

The performance of the proposed APF depends on the following three basic circuits:

1- The control circuit.

2- The drive circuit.

3- The power circuit.

The control circuit of this filter splits the load current into two components; the active component $i_a(t)$ and the reactive and harmonic component $i_{th}(t)$. The reference current $i_{th}(t)$ is extracted from the load current by subtracting the estimated active component $i_a(t)$ from the load current.

In the control circuit, the obtained reference current is directly compared with a triangular carrier signal to generate the switching patterns for the injected current. This can be easily performed by the drive circuit. The power circuit is operated according to the required switching patterns and converts a dc voltage of the voltage source inverter into PWM current that is injected into the ac lines to cancel the harmonic and

Using equations (5) and (6), yields:

$$\frac{I_a(S)}{I_l(S)} = \frac{\frac{\alpha^2 K_P}{T_o} S + \frac{\alpha^2 K_I}{T_o}}{S^2 + \frac{1}{T_o}(\alpha^2 K_P + 1)S + \frac{\alpha^2 K_I}{T_o}} \quad \ldots(7)$$

V. *The output voltage and current of the APF*

To study a three-phase system, it is converted to the equivalent single phase circuit and will be analyzed in the same method unless it is unbalance.

The output voltage of the APF that uses the PWM technique can be related to the modulating reference current as follows:
Because of the triangles similarity shown in Fig. 6, we can write

$$\frac{\tau}{T_s} = \frac{i_{rh}(t)}{A_c} \quad \ldots(8)$$

On the other hand, the dc value of the pulse in the output of the power inverter is directly proportional to the value of its duty cycles, so;

$$v_{inv.}(t) = V_{dc} \cdot \frac{\tau}{T_s} \quad \ldots(9)$$

Using equation (8) into equation (9) yields;

$$\frac{v_{inv.}(t)}{V_{dc}} = \frac{i_{rh}(t)}{A_c} \quad \ldots(10)$$

Then,

$$v_{inv.}(t) = \frac{V_{dc}}{A_c} \cdot i_{rh}(t) = M.i_{rh}(t) \quad \ldots(11)$$

where $M = V_{dc}/A_c$ and is called the modulation index.

It can be noticed from equation (11), that the desired value of the APF output voltage can be controlled by adjusting the modulation index.

Using the circuit of the single phase active power filter shown in Fig. 7, the equation that relates the proposed filter current and voltages (output voltage of the APF and the line voltage) can be expressed as:

$$\frac{di_F(t)}{dt} = \frac{1}{L_F}(v_{inv}(t) - v_S(t)) \quad \ldots(12)$$

By integrating both sides of the equation (12), the output current of the APF will be:

$$i_F(t) = \frac{1}{L_F}\int_o^t (v_{inv}(t) - v_S(t)) \quad \ldots(13)$$

Substituting for $v_{inv.}(t)$ from equation (11) into equation (13) yields:

$$i_F(t) = \frac{1}{L_F}\int_o^t (M.i_{rh}(t) - v_S(t)) \quad \ldots(14)$$

This current represents the injected compensating current to ac line.

VI. Simulation Results

(a) Election of parameters:

The parameters of the low pass filter, P-I controller and analog multiplier were selected to give a good compromise between output overshoot and settling time. Choosing the scaling factor of the analog multiplier (α) as 1V/V and time constant of the low-pass filter (T_o) as 0.094 sec. (i.e. the cut-off frequency of 10 Hz) gives a good attenuation for frequencies equal or greater than the mains frequency. The filtering characteristics of the low pass filter is shown in Fig.8.

Simulation studies for different values of the proportional parameter K_P and integral parameter K_I of the P-I controller are illustrated in the curves of Figs. 9 and 10 respectively. From Fig. 9, it is clear that optimal response of the system is obtained with $K_P = 35$. Also, the effect of the another coefficient (integral parameter K_I) on the response is investigated using Fig. 10, where good stability of the system is obtained with $K_I = 400$ for the considered specifications.

Finally, the consequence of electing the optimal values for K_P and K_I is shown in Fig.11. Where the response of the P-I controller reaches its steady-state value in about two cycles without any overshoot in the current amplitude.

(b) The stability test:

Using the selected values for α, T_o, K_P and K_I in equation (7) yields equation (15):

$$\frac{I_s(s)}{I_L(S)} = \frac{372.978S + 4255.32}{S^2 + 382.978S + 4255.32} \quad ...(15)$$

The Routh and Herwitz criteria has been used to investigate stability of the analyzed system. Where for stability reasons, the Routh table for stability of characteristic equation and also this equation has only positive coefficients, then it is always stable [8].

(c) Load tests:

Fig. 12 shows the response of the control circuit for a change in the magnitude of the load current with unity power factor. A change in the magnitude will produce momentary harmonic current and distortion in the active current as illustrated in this figure. Fig. 13 illustrates the key waveforms for a load current with displacement of 90° lagging whereas Fig. 14 shows the 90° leading. A simulation of load current with high order of harmonics is illustrated in Fig. 15.

To investigate the ability of the designed control scheme in operating at other frequency and giving the same characteristics as when it is working at 50 Hz, simulations have been carried out to operate the control circuit at 40 Hz and 60 Hz mains frequency. Figs. 16 and 17 have illustrated this ability.

To subject the control circuit to a worst case, the magnitude and frequency of the load current have been changed at the same time. Figs. 18 and 19 show that the control circuit can perform its job efficiently.

VII. Experimental Results

To verify the characteristics and performance of the designed active power filter, a prototype system has been constructed and tested. Several tests have been implemented in order to confirm the effectiveness of the active power filter. These tests include:

a) Inductive load test

The active power filter has been used to compensate the reactive power for different lagging load power factor and the results of such compensate are summarized in Table .1, these results shows that approximately unity power factor at the mains can be obtained using the designed APF

Table1:Inductive load test

MAINS		*LOAD*	
Phase angle (deg.)	*Power factor (cosϕ)*	*Phase angle (deg.)*	*Power factor (cosϕ)*
0	1.000	0	1.000
2	0.999	10	0.984
2.5	0.999	20	0.939
3.5	0.998	30	0.866
3.5	0.998	40	0.766
5	0.996	50	0.642
5	0.996	60	0.500
7	0.992	70	0.342

The practical waveform of load voltage, load current, mains voltage and mains current are as in the Fig. 20a.

a) Capacitive load test

The results of the compensation for a capacitive load with different values of power factor as summarized in Table.2. These results also, confirm the effectiveness of the filter in compensating the capacitive reactive power.

Table 2: Capacitive load test

MAINS		LOAD	
Phase angle (deg.)	Power factor (cosϕ)	Phase angle (deg.)	Power factor (cosϕ)
0	1.000	0	1.000
2.5	0.999	10	0.984
2.5	0.999	20	0.939
2.5	0.999	30	0.866
3	0.998	40	0.766
3	0.998	50	0.642
4	0.997	60	0.500
6	0.994	70	0.342

Figure.20b illustrates the experimental waveform of load voltage, load current, mains voltage and mains current.

a) The harmonic cancellation

The second objective of the active power filter has been verified with the bridge rectifier used as a nonlinear load. The result is that the mains current has been made sinusoidal wave and the mains power factor has become unity.

Figs.21a and 21b show the load voltage, load current, mains voltage and mains current for two cases; the first when the dc load of the bridge rectifier has inductive filtering and the second when the output filter is a capacitive.

VIII. *Conclusions*

In this paper, a three – phase active power filter have been studied and implemented. The proposed scheme employs a pulse-width modulation voltage source inverter to compensate the reactive power requirement of the load current and eliminate the harmonic contamination caused by the nonlinear loads. Hence, the supply current will be a pure sinusoidal and in-phase with the supply voltage whatever is the type of the load.

The electronic circuits used in implementation of the control circuit (such as PLL and multiplier circuits) are simple, accurate and have a fast response making an overall time response of about two cycles of the fundamental. Hence, simplicity, low cost and fast response are the main features of the implemented control circuit.

The tests carried out on the implemented APF have shown that its output current is effective in compensating the reactive and harmonic content of the load current for all the considered types of load (linear and nonlinear with different power factor). Almost unity power factor and sinusoidal mains current has been obtained for the different types of loads used in these tests.

The close agreement between analytical and experimental results proves the validity of the analysis and the feasibility of the proposed system.

IX. *References*

[1]:Peter Lynch, "An active approach to harmonic filtering", IEE REVIW, pp. 128-130, May 1999.

[2]: Tashihiko Noguchi, Hiroaki Tomiki, Seiji Kondo, and Isao Takahashi, " Direct power control of PWM converter with out power-source voltage sensors", IEEE Transactions on Industry Applications, vol. 34, no.3,pp. 473-479, May/June 1998.

[3]: J. Sebastian Tepper, Juan W. Dixon, Gustavo Venegas, and Luis Moran, "A simple frequency-independent method for calculating the reactive and harmonic current in a nonlinear load", IEEE Transactions on Industrial Electronics, vol. 43, no. 6, pp. 647-653, December 1996.

[4]: P. Verdelho, and G. D. Marques, "An active power filter and unbalance current compensator", IEEE Transaction on Industrial Electronics, vol. 44, no 3, pp. 321-328, 1997.

[5]: Juan W. Dixon, Gustavo Venegas, and Luis Moran, " A series active power filter based on a sinusoidal current-controlled voltage source inverter", IEEE

Transactions on Industrial Electronics, vol. 44, no. 5, pp. 612-919, October 1997.

[6]: Luis A. Moran, Luciano Fernandez, Juan W. Dixon, and Rogel Wallace, "A Simple and low cost control strategy for active power filters connected in cascade" IEEE Transactions on Industrial Electronics, vol. 44, no. 5.pp. 621-629, October 1997.

[7]: W.M. Grady, M.J. Samotyj, and A.H. Noyola, "Survey of active power line conditioning methodologies", IEEE Transactions on Power Delivery, vol.15, no.3, pp.1536-1542, July 1990.

[8]:I.J.Nagrath, and M. Gopal,"Control systems engineering", New Age International Publishers, New Delhi, 3rd edition,2000.

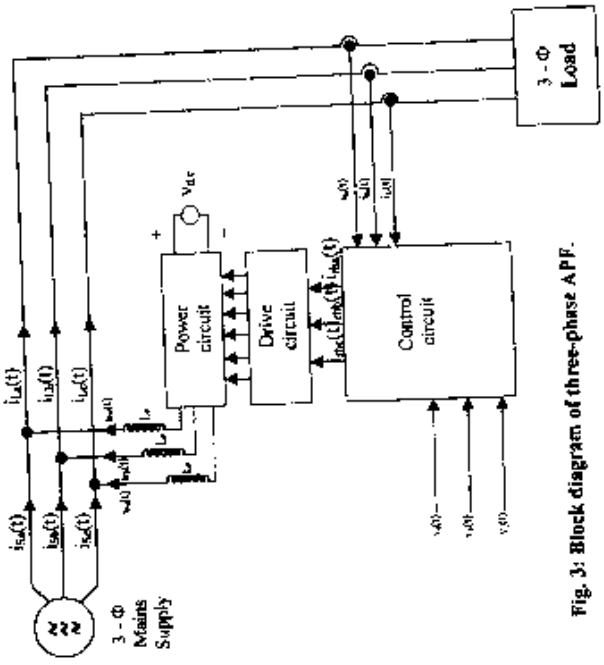

Fig. 3: Block diagram of three-phase APF.

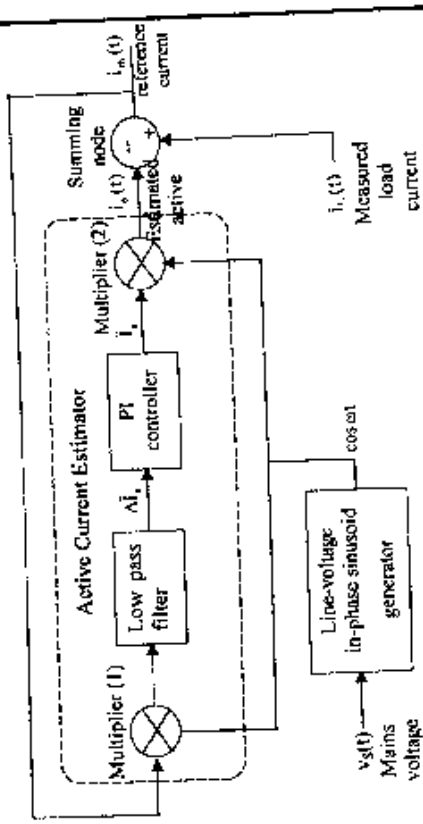

Fig. 4: Block diagram of the control circuit for APF (one phase).

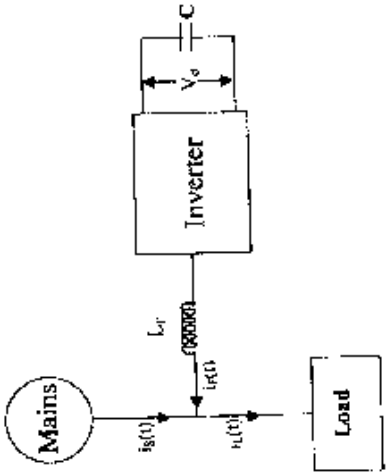

Fig. 1: Voltage source inverter APF.

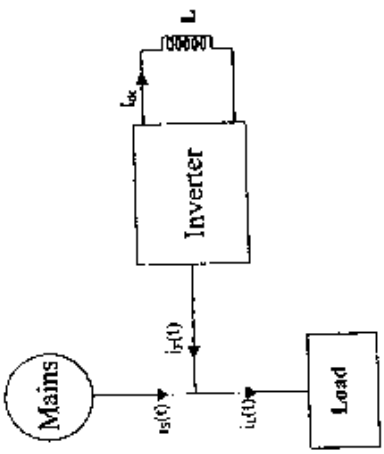

Fig. 2: Current source inverter APF.

Vol. 1, No.1, 2005

Fig. 5: Closed loop of the control circuit in a S-domain (one phase).

Fig. 6: Time diagram illustrating the PWM strategy.

Fig. 7: The single phase PWM – VSI active power filter.

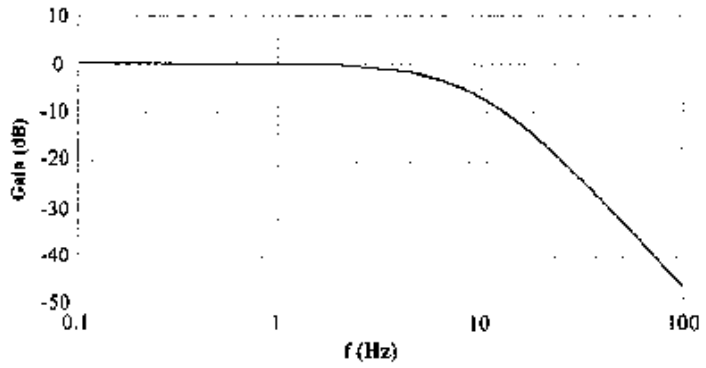

Fig. 8: Filtering characteristics

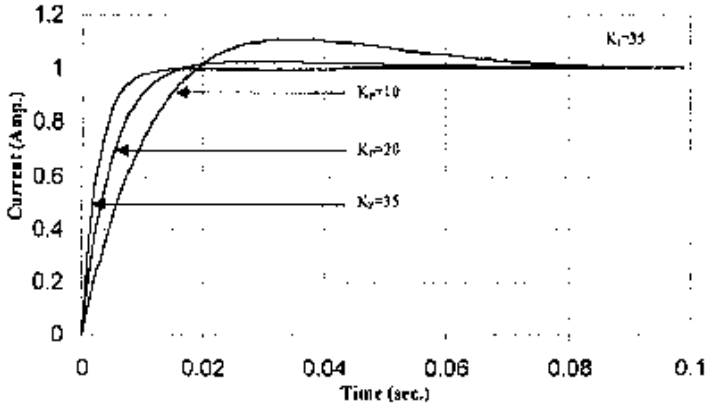

Fig. 9: Response of the closed loop circuit, unit step input with variation of K_P.

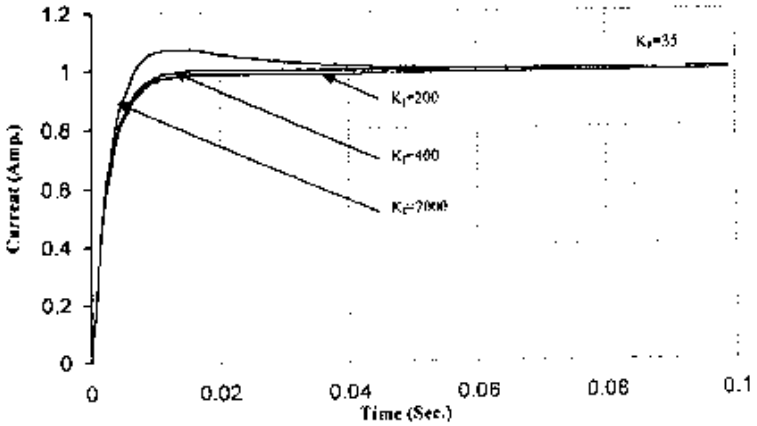

Fig. 10: Response of the closed loop circuit, unit step input with variation of K_I.

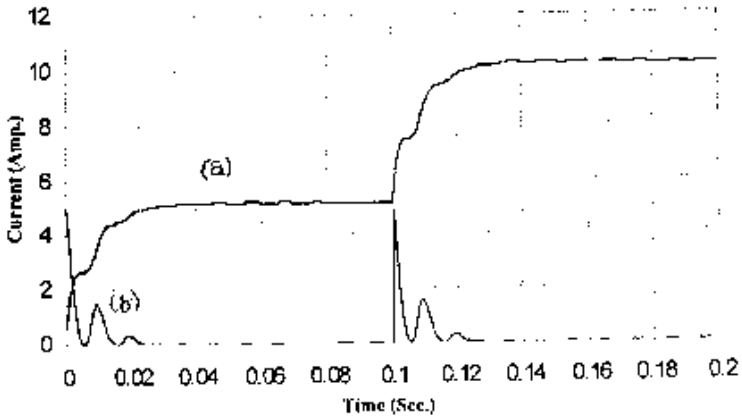

Fig. 11: (a) P-I controller response for current load change at unity power factor.
(b) Output of the first multiplier

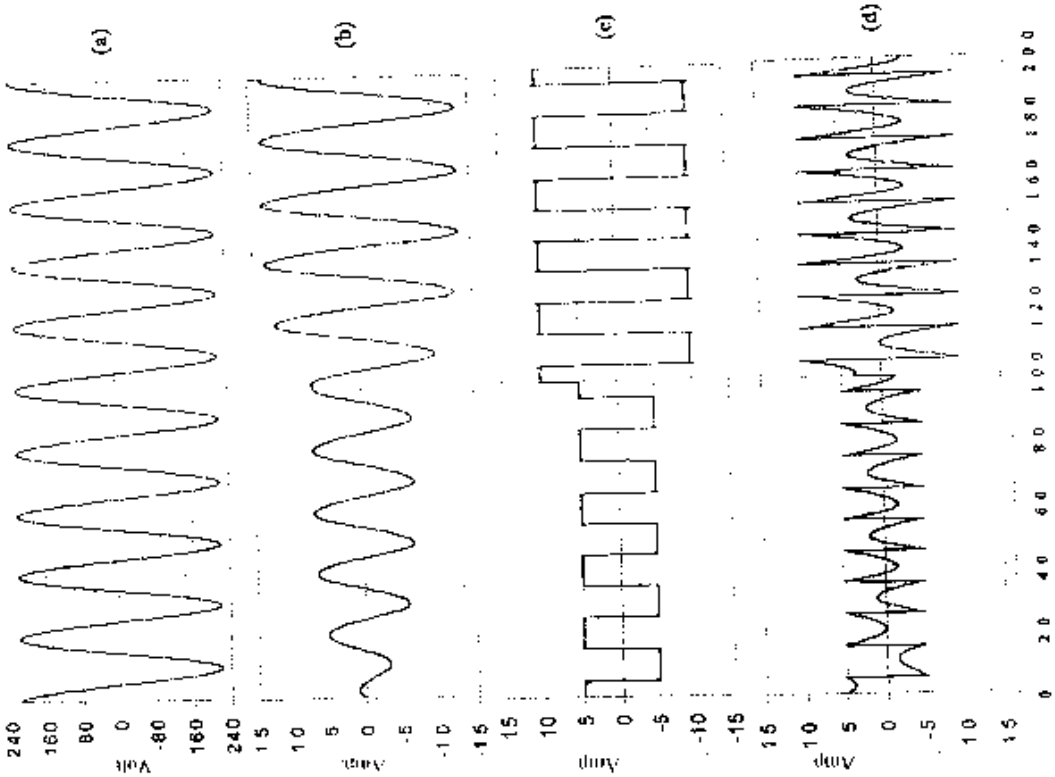

Fig. 13: Simulation results with rectifier load (50 Hz). (a) Mains voltage $v_s(t)$, (b) Estimated current $i_s(t)$, (c) Load current $i_L(t)$, (d) Reference current $i_{ref}(t)$

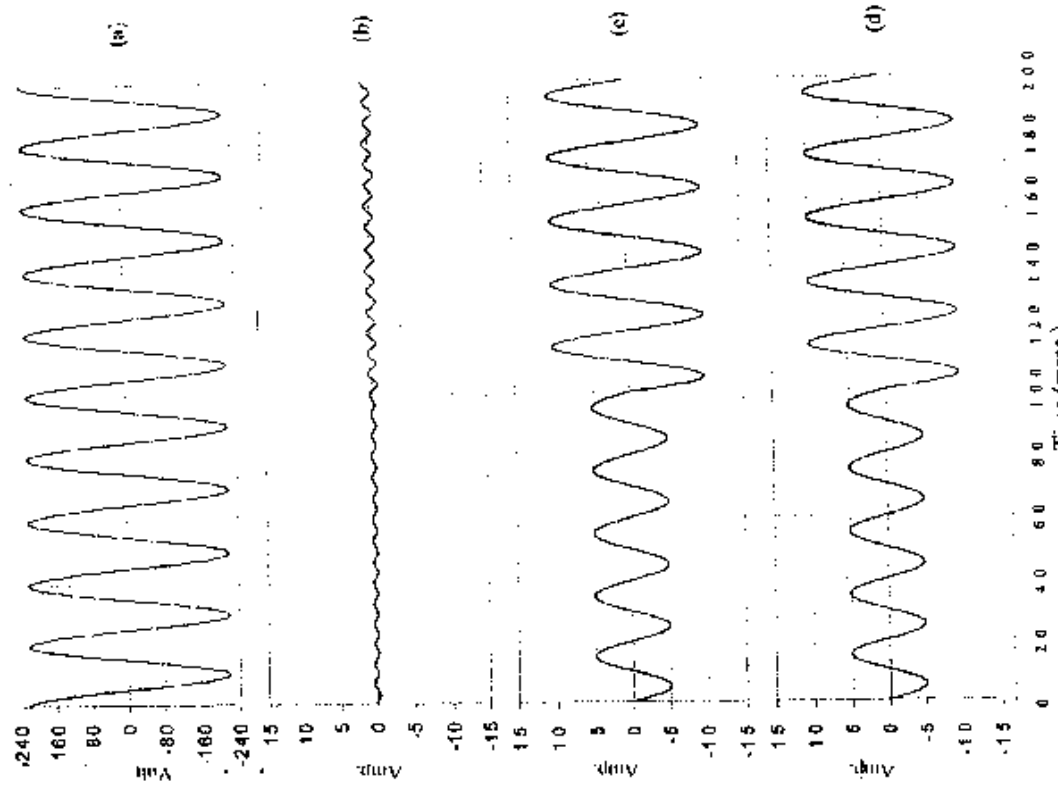

Fig. 14: Simulation results at $\theta = 90^{\circ}$load (50 Hz). (a) Mains voltage $v_s(t)$, (b) Estimated current $i_s(t)$, (c) Load current $i_L(t)$, (d) Reference current $i_{ref}(t)$

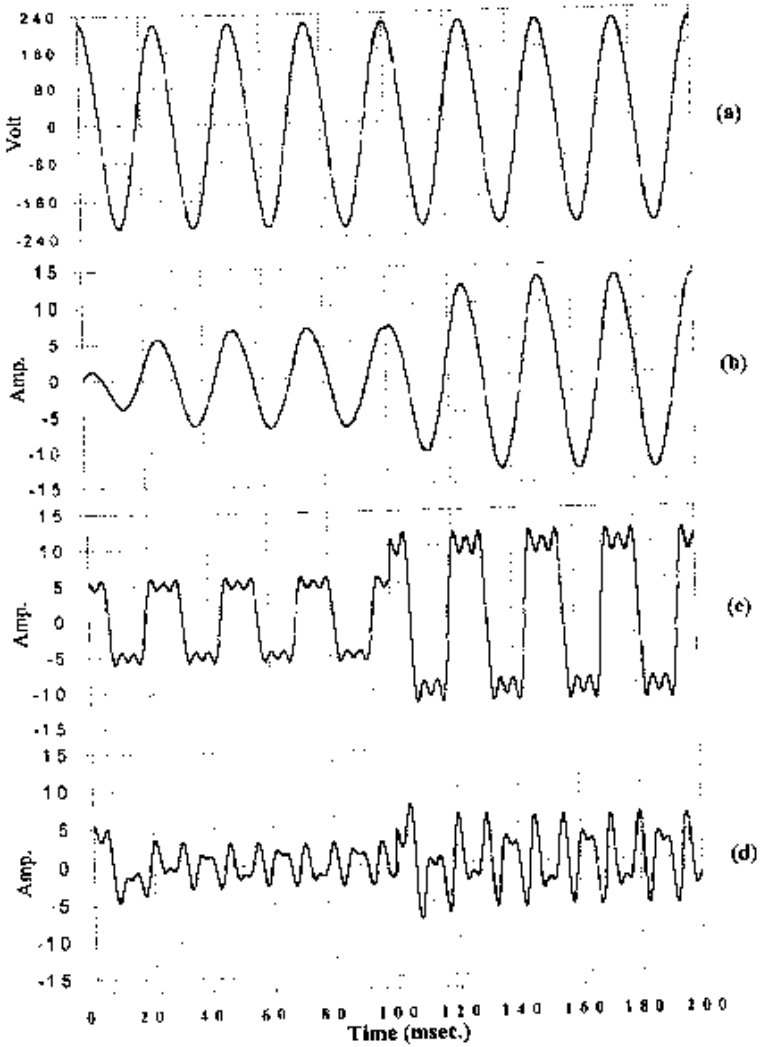

Fig.(16): Simulation results for rectifier load, f_s=40 Hz. (a) Mains voltage $v_s(t)$, (b) Estimated current $i_e(t)$, (c) Load current $i_l(t)$, (d) Reference current $i_{re}(t)$

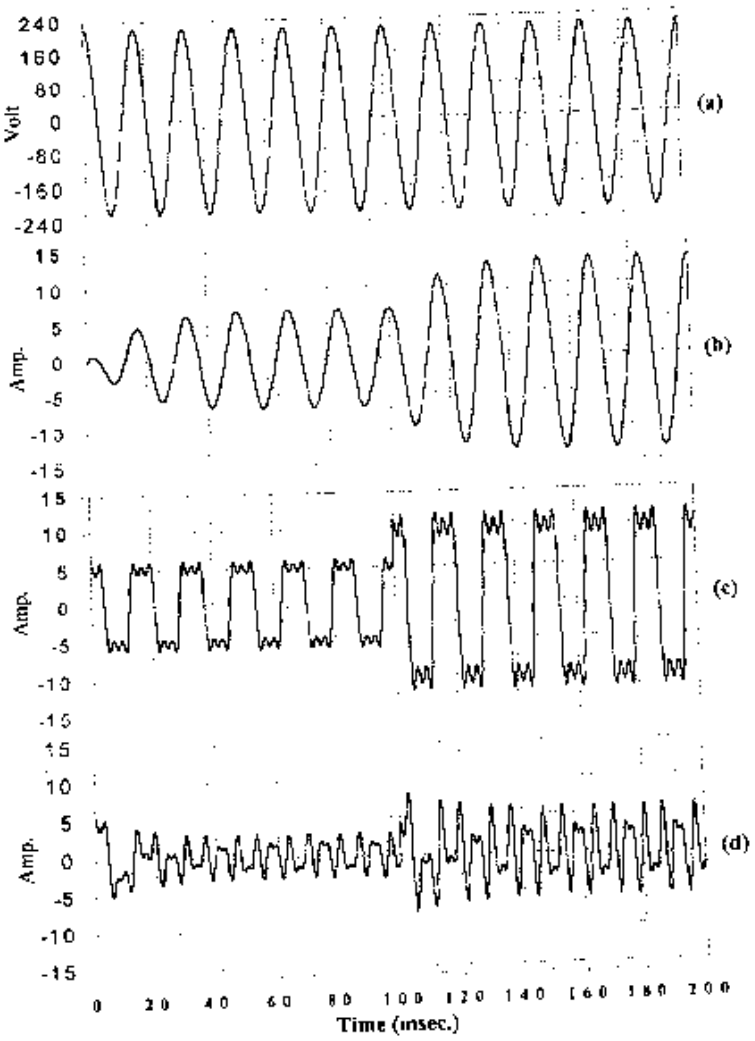

Fig.(17): Simulation results for rectifier load, f_s=60 Hz. (a) Mains voltage $v_s(t)$, (b) Estimated current $i_e(t)$, (c) Load current $i_l(t)$, (d) Reference current $i_{re}(t)$

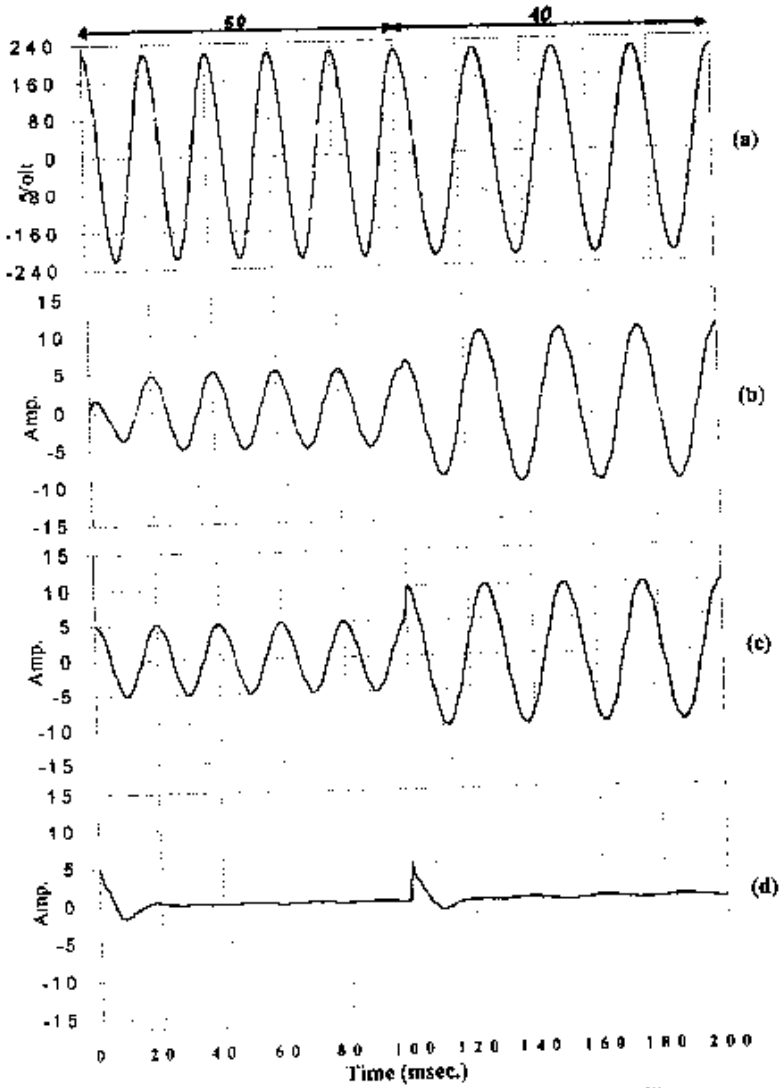

Fig.(18): Simulation results for θ = 0 °. (a) Mains voltage $v_s(t)$, (b) Estimated current $i_a(t)$, (c) Load current $i_l(t)$, (d) Reference current $i_{ra}(t)$.

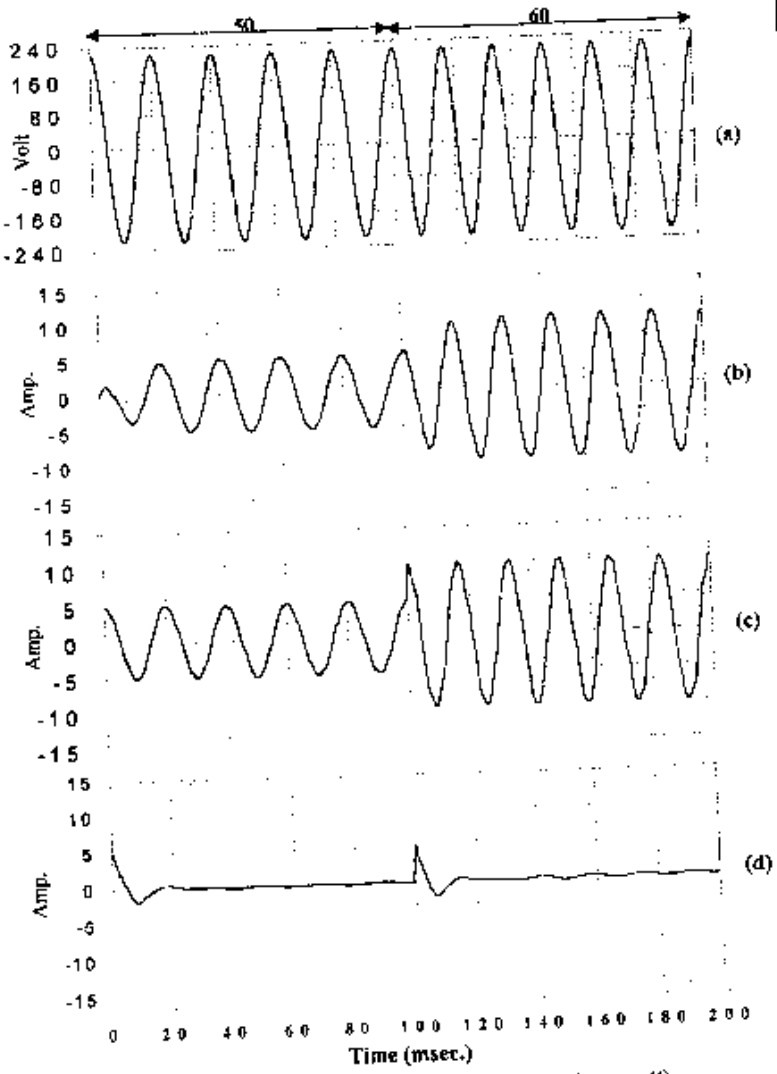

Fig.(19): Simulation results for θ = 0 °. (a) Mains voltage $v_s(t)$, (b) Estimated current $i_a(t)$, (c) Load current $i_l(t)$, (d) Reference current $i_{ra}(t)$.

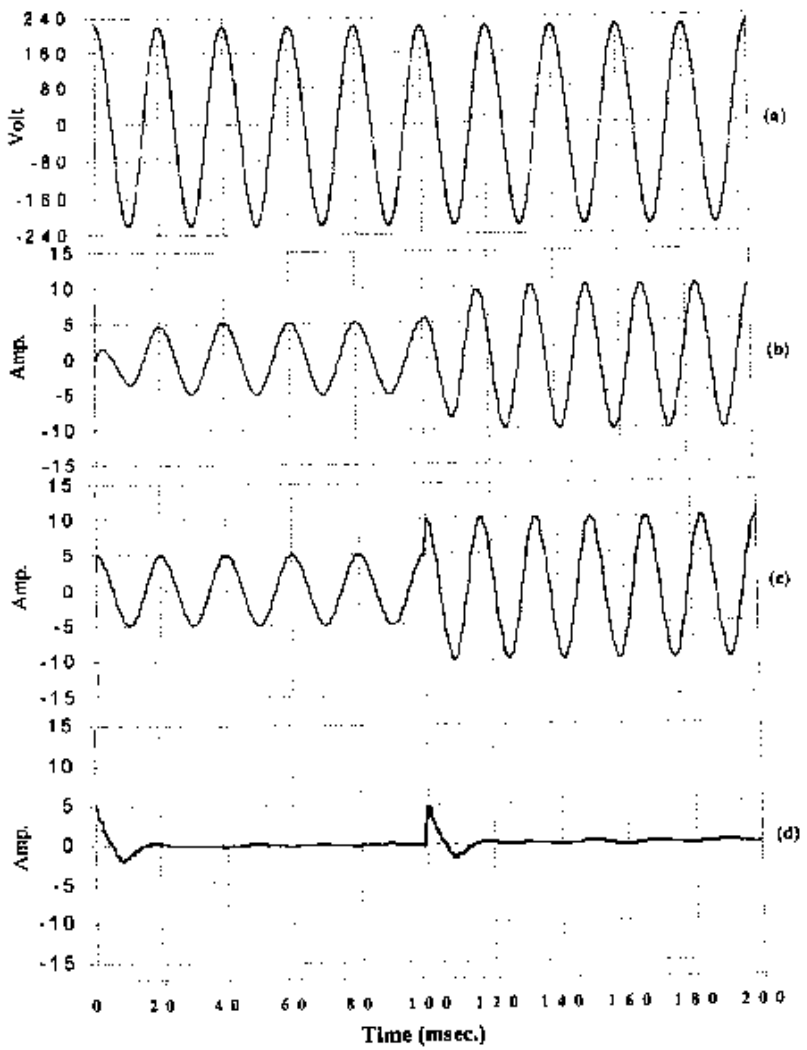

Fig.(12): Simulation results for θ=0 °,f_s= 50 Hz. (a) Mains voltage $v_s(t)$, (b) Estimated current $i_a(t)$, (c) Load current $i_l(t)$, (d) Reference current $i_{rh}(t)$.

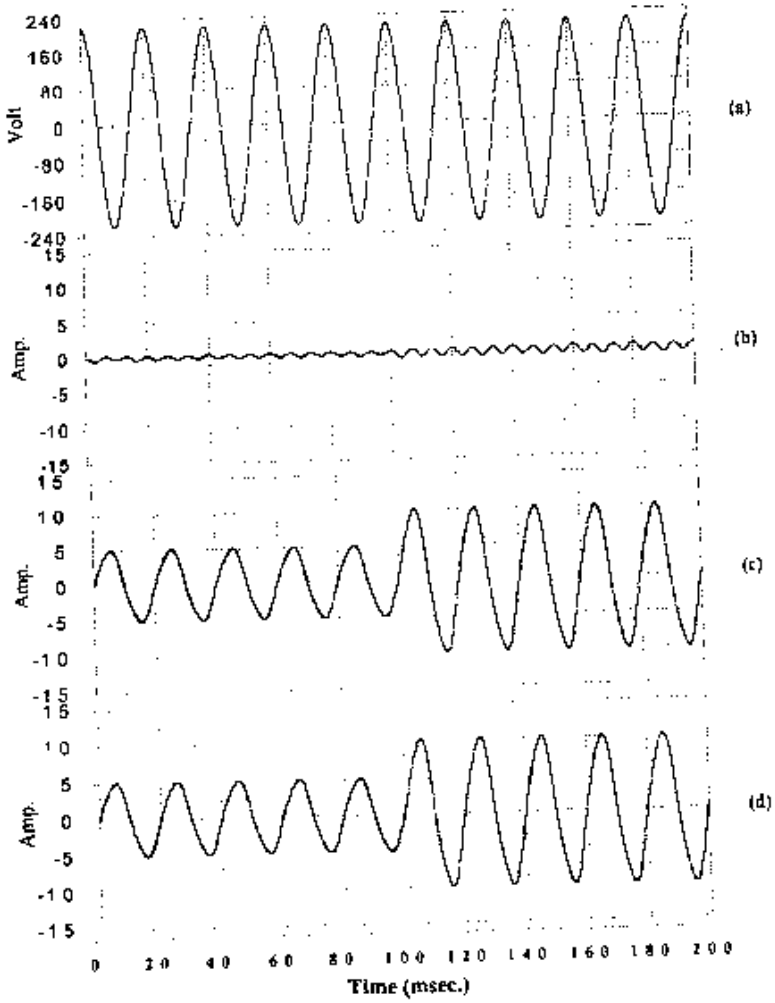

Fig.(13): Simulation results for θ=90° lag, f_s= 50 Hz. (a) Mains voltage $v_s(t)$, (b) Estimated current $i_a(t)$, (c) Load current $i_l(t)$, (d) Reference current $i_{rh}(t)$.

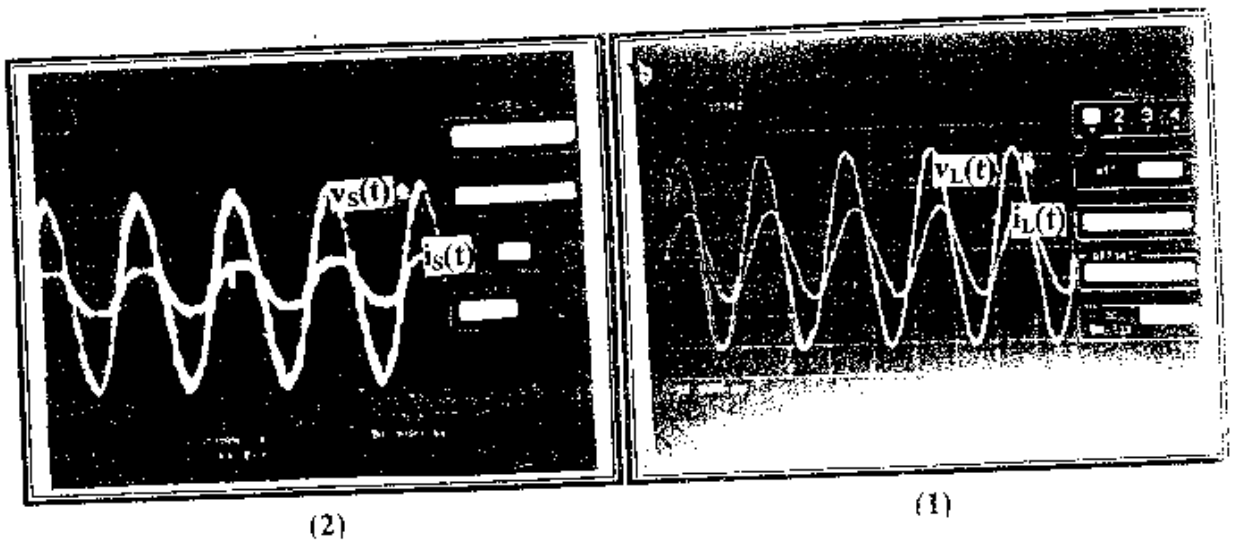

(2) (1)

(a)

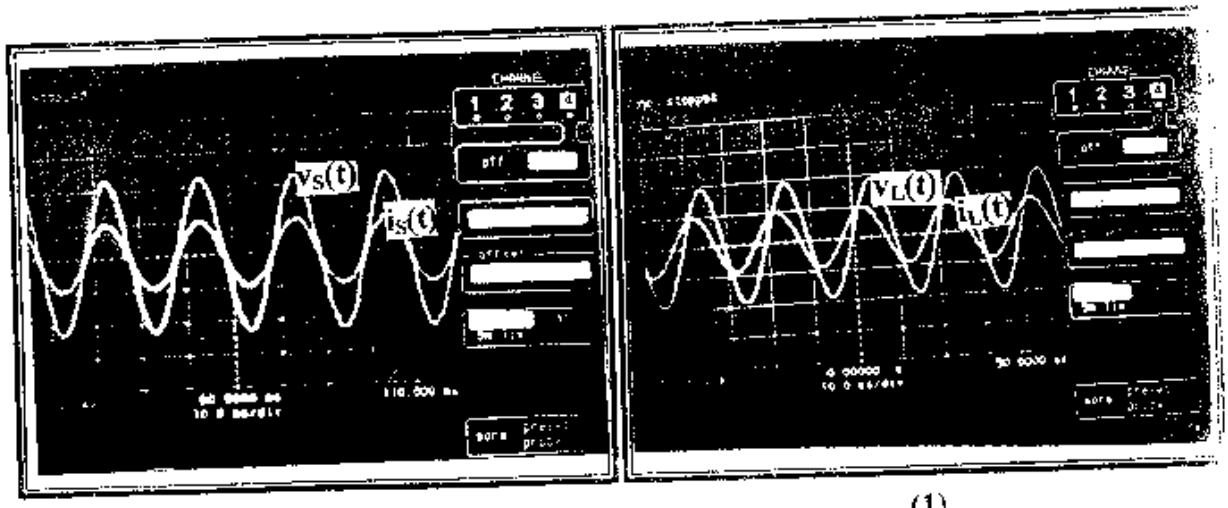

(2) (1)

$v_S(t)$, $v_L(t)$ 20V/div. (b) $i_S(t)$, $i_L(t)$ 1A/div.

Fig. 20: Reactive power compensation performance. (10 msec./div.)
(1) Current and voltage of the load.
(2) Current and voltage of the mains supply.
(a) Inductive load test. (b) Capacitive load test.

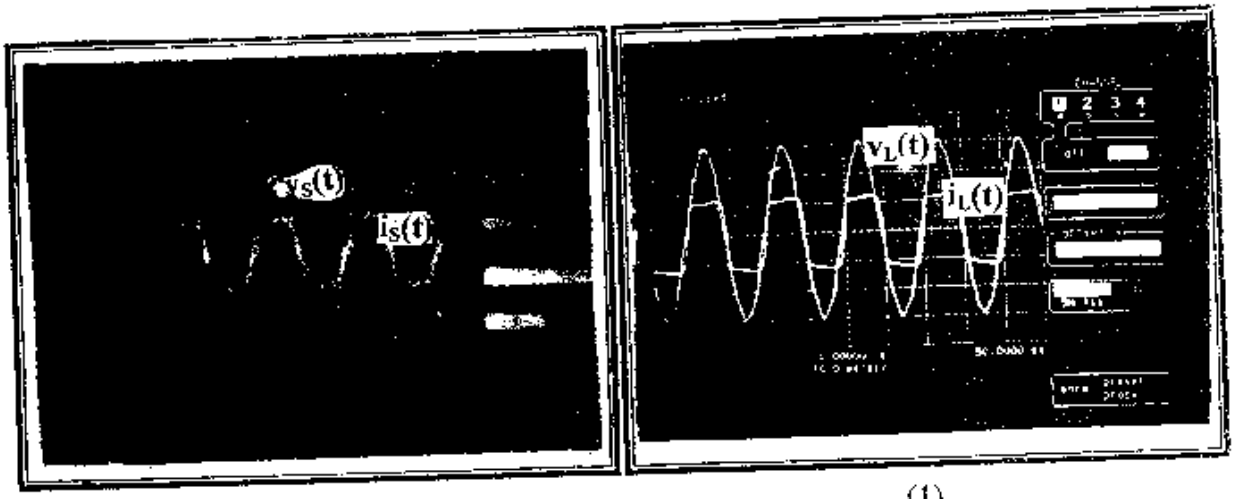

(2) (1)

(a)

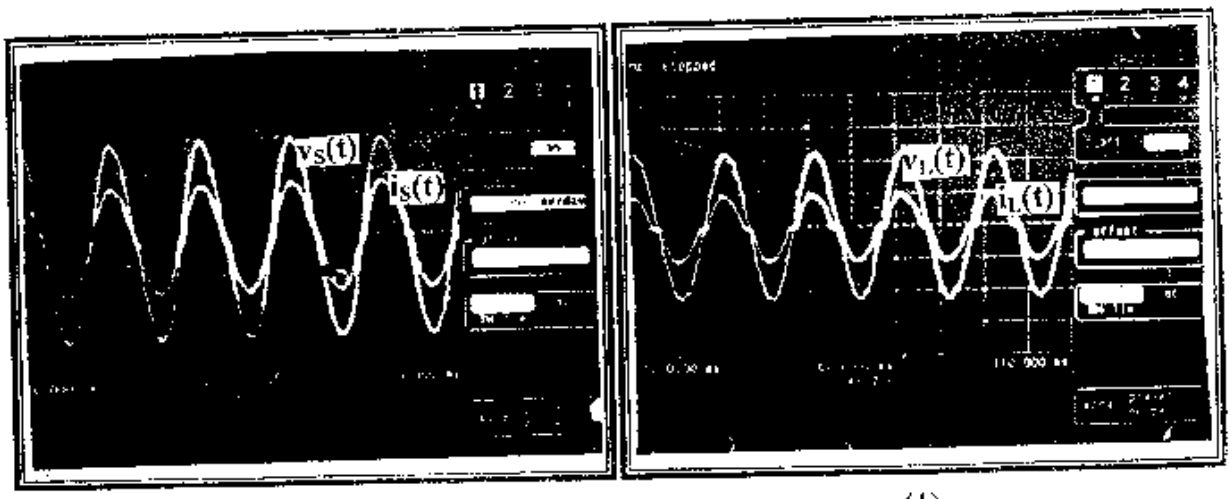

(2) (1)

$v_S(t)$, $v_L(t)$ 20V/div. (b) $i_S(t)$, $i_L(t)$ 1A/div.

Fig. 21: Harmonics cancellation performance. (1) current and voltage of the load.
(2) current and voltage of the mains supply.
(a) full wave diode rectifier with R-L load in dc side.
(b) full wave diode rectifier with R-C load in dc side.